Fall 2010

Gas evolution of corn kernels, oat hulls, and paper sludge from biomass gasification

James Steven Ulstad
University of Iowa

GAS EVOLUTION OF CORN KERNELS, OAT HULLS, AND PAPER SLUDGE FROM BIOMASS GASIFICATION

by

James Steven Ulstad

A thesis submitted in partial fulfillment
of the requirements for the Master of
Science degree in Mechanical Engineering
in the Graduate College of
The University of Iowa

December 2010

Thesis Supervisor: Assistant Professor Albert Ratner

Graduate College
The University of Iowa
Iowa City, Iowa

CERTIFICATE OF APPROVAL

MASTER'S THESIS

This is to certify that the Master's thesis of

James Steven Ulstad

has been approved by the Examining Committee for the thesis requirement for the Master of Science degree in Mechanical Engineering at the December 2010 graduation.

Thesis Committee: _____
Albert Ratner, Thesis Supervisor

_____
James Buchholz

_____
H. S. Udaykumar

ACKNOWLEDGMENTS

The author would like to thank Professor Albert Ratner for his time, guidance, and support as well as Jean Dochterman, Brian Sulak, and John Hennigan for their assistance in all facets of this project. Also, The University of Iowa Power Plant, under the supervision of Ferman Milster, for their funding and support.

ABSTRACT

Gasification of biomass has become an area of key interest as it is a reasonably quick and direct way of converting material into a fuel source that works in many industrial systems. The purpose of the present work is to explore biomass gasification and in particular pyrolysis behavior of corn kernels, oat hulls, and paper sludge. For the materials, low temperature gasification behavior was studied. Here, tests were performed with pyrolysis temperatures from 400 - 800°C, at 1 atm and a rapid heating rate. A small concentration of O_2 was added to the gasification agent (N_2) to enhance CO yields, similar to modern industrial gasifiers. The evolution of CO, CO_2, CH_4, H_2, and O_2 were measured throughout the pyrolysis process. Results show a direct correlation between temperature and the composition of the gas byproduct for all biomasses. CO production increases with an increase in temperature while CO_2 shows no temperature correlation. O_2 depletion mimics the CO evolution and increases with an increase in temperature. CH_4 production was observed, however the results were rarely repeatable due to the sensor's sensitivity to moisture and tar in the gas byproduct. No hydrogen was observed, as would be expected for the short experimental residence time (0.2 seconds).

TABLE OF CONTENTS

LIST OF TABLES

LIST OF FIGURES

CHAPTER 1

INTRODUCTION AND LITERATURE REVIEW

This work explores the process of biomass gasification, a process which uses solid or liquid biomass to create energy through incomplete combustion. Currently, most of the world relies on non-renewable fossil fuels. Fossil fuels used for energy production, such as coal, release carbon dioxide (CO_2) and sulfur (S) into the atmosphere that previously had been compressed and stored underneath the earth for ages. Biomass gasification uses biomass, biological material from living or recently living organisms, and converts it into carbon monoxide (CO), hydrogen (H_2), and methane (CH_4) which can later be processed into liquid fuel or electrical energy. Through gasification, the CO_2 originally absorbed by the biomass is re-released into the atmosphere making it a carbon neutral process (i.e. no additional CO_2 is released). For these reasons and many more, gasification has become an attractive option for power production and it is currently being used and studied at The University of Iowa. By co-firing The University of Iowa's Main Power Plant (UIMPP) boilers with oat hulls and coal, the UIMPP reduces their annual coal usage by 20,000 tons. More importantly, the annual CO_2 emissions have been decreased by ~60,000 tons (the equivalent of removing 1,200 passenger vehicles from the road each year) and the University has saved over $2.45 million dollars with this project [1]. The oat hulls used at the UIMPP are a byproduct of cereal making processes and were purchased from Quaker Oats for a fraction of the cost of coal. Over 160 tons of oat hulls are delivered to the University by Quaker Oats each day which reduces Quaker Oats' costly waste disposal fees and Iowa landfill space. Due to the great success of the partnership between The University of Iowa and Quaker Oats, this manuscript attempts to

develop a greater understanding of the gasification process, in particular the pyrolysis of numerous materials, and to gather experimental data that can used to create better gasification models, further advancing the understanding of this necessary renewable energy process. Hopefully, by developing a larger knowledge base for the gasification process, The University of Iowa and other entities can better embrace this carbon neutral process by making it more economical and environmentally friendly.

1.1 Gasification Processes

The global gasification processes (from biomass to usable energy) can be categorized as upstream processing, gasification, and downstream processing as seen in Figure 1.1 [2]. Upstream processing, or preprocessing, is where the biomass is made suitable for gasification by reducing the particle size. Gasification is the most important process and is where biomass is converted into gaseous products, known as syngas, pyrolysis gas, or gasification gas, and is composed mostly of CO, CO_2, CH_4, H_2, H_2O, and traces of other heavier hydrocarbons. The two main processes associated with downstream processing include gas clean-up and utilization. In the gas clean-up process, tars and other contaminates (alkalis, nitrogen, and sulfur) are removed from the syngas prior to energy conversion in the gas utilization process.

The gasification process is the heart of the *global* biomass gasification process and is the focus of this manuscript. Within the gasification process, three stages occur [3]:

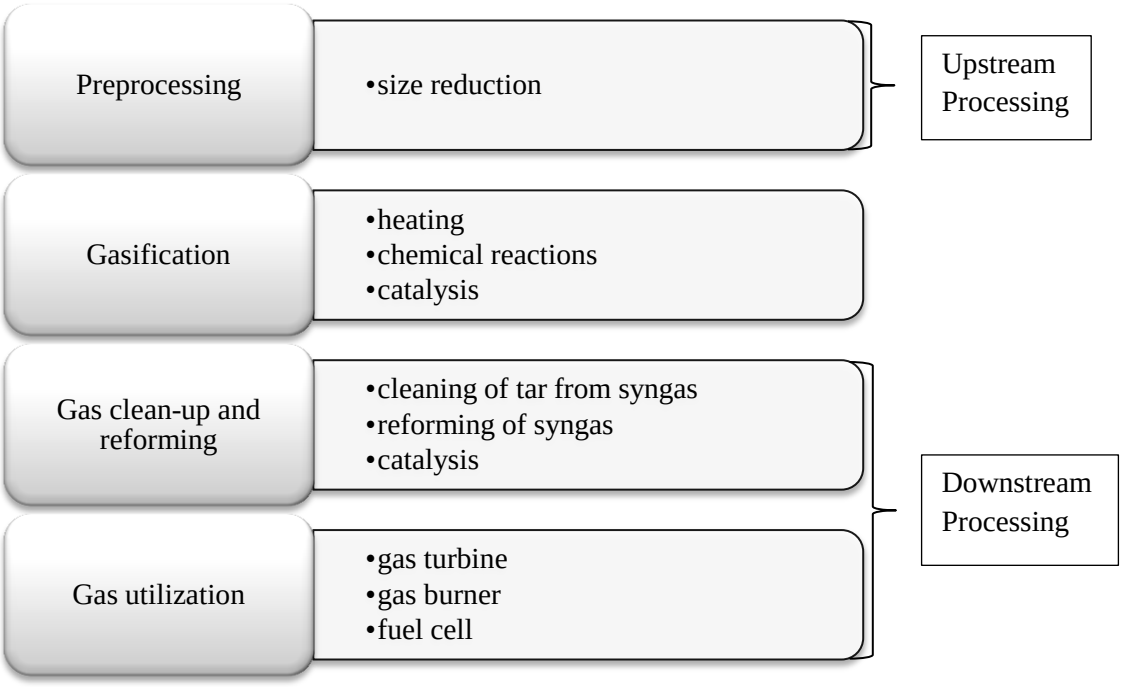

Figure 1.1: Biomass gasification processes

- Pre-heating and drying
- Pyrolysis
- Char gasification and char oxidation

The three stages of gasification occur simultaneously, however, no sharp boundaries exist, causing overlap to the point where all three stages can occur simultaneously. This overlapping effect is quite complex and results in extreme modeling difficulty. Within the pre-heating and drying stage, moisture contents in the biomass are removed and produce a syngas with a higher heating value. Pyrolysis is where the majority of the biomass is decomposed into solid char, volatiles (condensable hydrocarbon or tar) and gases. Also, during pyrolysis, most of the contents containing a vast majority of the energy are released over a few minutes. Little to no data exists which focus directly on biomass pyrolysis and has been assumed to be instantaneous in some models [4] even

though it is a significant stage taking a considerable amount time throughout the gasification process. This work focuses on developing a greater understanding of biomass pyrolysis, specifically the instantaneous release of the permanent gases (CO, CO_2, CH_4, O_2, and H_2) in order to create reduced numerical reaction models which can later be used in CFD models. Ideally, accurate estimations of the gasification stages would significantly aid in gasification simulations by simplifying the complex process into simple numerical models associated with the materials and/or the material makeup. This simplification would reduce simulation setup and computation times making the gasifier design and simulation processes more efficient and useful.

The third stage, char gasification and oxidation are one of the most important steps of the gasification process and have been studied intensely however it is not the focus of this work. Char breakdown during this stage is crucial to gasifier performance even though the majority of the mass fraction of the fuel is produced in the pyrolysis stage [3]. Reactor size and gasification efficiency are determined by the extent and rate of char gasification. Due to this, most gasification models can be more accurately described as char gasification models.

1.2 Types of Gasifiers

Modern gasifiers have two main classifications: fixed and fluidized beds [2, 3, and 5]. Fixed bed gasifiers are the simpler of the two and have two major designs: updraft and downdraft. In updraft gasifiers, biomass feeds are injected through the top of the gasifier while air at ~1300°C enters through the bottom, gasifying the biomass as it falls through the gasifier as seen in Figure 1.2. The products of gasification then exit through the top to be further processed. Gasification zones within the updraft gasifier can

also been seen in Figure 1.2 as the biomass is converted into syngas. First the moisture is removed in the drying zone followed by pyrolysis where a majority of the volatiles are released. In the reduction and combustion zones the char is broken down. Steam used as the reactive or gasifier agent is commonly associated with this gasifier type. Low density and/or fluffy biomasses are unsuitable for use in an updraft gasifier due to the high ash production commonly associated with low densities and small particle sizes [5].

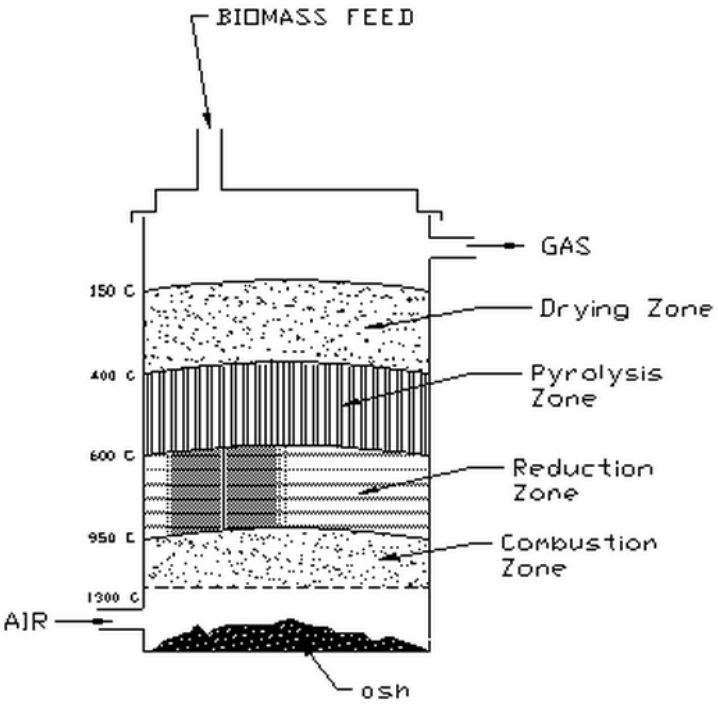

Figure 1.2: Updraft fixed bed gasifier [5]

Downdraft gasifiers are similar to updraft gasifiers however the gasification zones are reversed. Fuel is again introduced through the top while the gasifying agent is introduced through the side. The main difference is the location of the gas outlet near the bottom of the gasifier as opposed through the top for an updraft gasifier. As a result of the syngas exiting through the bottom, less tar is produced from the product gas flowing

through the hottest region of the gasifier, the bed, reducing the necessary cleaning [2 and 5].

Fluidized bed reactors contain heated beds that transfer heat to the biomass along with the gasifying agent to create syngas as seen in Figure 1.3. The bed is commonly made of inert material such as sand or ash and the fuel feed is introduced through the bottom [5]. No distinct gasifying zones exist causing the gasification and pyrolysis to occur simultaneously throughout the gasifier, enhancing the heat transfer and increasing reaction rates and conversion efficiencies [2]. Catalysts may also be added which can increase the gasifier efficiency, alter syngas yields, and reduce tar production. Common catalysts include: carbonates, limestone, calcium chloride, and inorganic salts. Complicated controls systems cause these gasifier types to only be viable at larger, industrial sizes (>30 MW thermal output) [5].

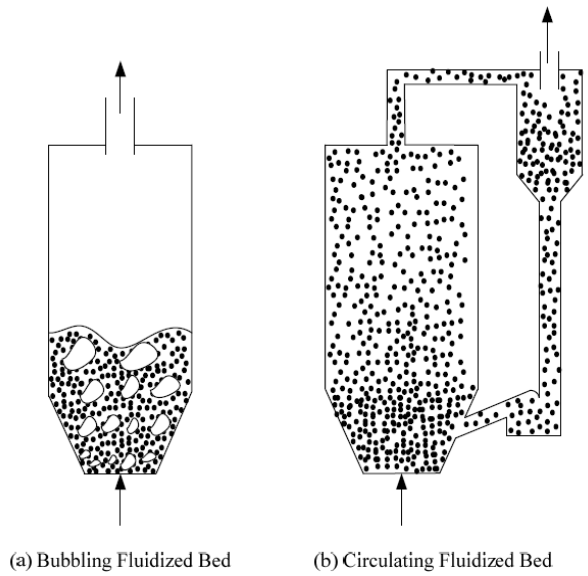

Figure 1.3: Fluidized bed gasifier types [3]

1.3 Fast/Rapid Pyrolysis

Pyrolysis is the gasification process where the majority of the volatiles are released through thermal decomposition of the fuel (biomass). Pyrolysis can be categorized by the temperature of the reaction and the speed at which it occurs. Three major pyrolysis types exist and can be seen in Table 1.1. Fast pyrolysis with a rapid heating rate was explored in this work and is of particular interest due to the products produced being similar to modern day fossil fuels [5].

Table 1.1: Pyrolysis types and properties

Pyrolysis Type	Heating Rate	Gas Residence Time	Average Temperature
Slow Pyrolysis	0.1 - 2°C/s	>5 seconds	500°C
Flash Pyrolysis	>2°C/s	<2 seconds	400 - 600°C
Fast Pyrolysis	200 – 10^5 °C/s	<2 seconds	>550°C

The kinetics of fast pyrolysis is of particular interest in modeling at reactor temperatures < 800°C where equilibrium modeling is not applicable (*See Section 1.8*) [3]. Heating rate, reactor temperature, pressure, ambient atmosphere, catalysts, and biomass composition have all be shown to affect the kinetics of the pyrolysis reactions [5]. Equation 1.1 summarizes the kinetics of fast pyrolysis where W_t is the particle weight, t is the pyrolysis time, W_∞ is the ultimate particle weight, K_o is the frequency factor in seconds, R is the universal gas constant, E is the activation energy, and T is the temperature.

$$\frac{dW_t}{dt} = K_o(W_\infty - W_t)exp^{\left(\frac{-E}{RT}\right)} \tag{1.1}$$

1.4 Averaged vs. Instantaneous Results

In recent works, two methods have been used to measure the gas composition: averaged and instantaneous. Averaged outputs allow for high accuracy due to the steady state nature of the measurements. These results however, require a significant number of assumptions to be used in computer models. This work specifically focuses on instantaneous measurements that can be directly utilized to construct reduced chemistry models of the pyrolysis stage which are then employed in gasifier design.

1.5 Temperature Range

Typical gasification temperatures range from 600 - 1000°C [2], however little to no data exists at low temperatures with instantaneous outputs. However, numerous studies have examined the effect of temperature on the total gas yield and composition. Experiments were performed for temperatures between 800 - 1,000°C on a range of softwoods for small particle sizes (~0.5 mm) [6]. It was found that the product gas composition was not sensitive to the tested temperature range. Biomass gasification of palm oil was simulated for temperatures between 150-1,200°C and found that four temperature zones exist that affect the product gas composition [7]. From 400 - 800°C, the average concentration of numerous gaseous species (C, H_2O, CH_4, CO_2, CO, and H_2) was highly sensitive to the pyrolysis temperature. Low temperature (~600°C) gasification of manure was studied for a fluidized bed reactor using both steam and N_2 as the gasifying agents [8]. Total gas yield and composition was measured and it was found that the use of steam as the gasifying agent increased the ratio of H_2 to CO by decreasing CH_4 and CO due to the steam reforming and water-gas shift reactions. These results may be comparable to this work, however it neglects the instantaneous gasifier

outputs and only one temperature (600°C) was analyzed. For this work, instantaneous gasifier output temperatures from 400 - 800°C were analyzed due to the lack of experimental data and the high sensitivity of gas compositions in that range.

1.6 Gasification Reactions

As discussed before, several temperature zones exist for temperatures between 150 – 1,200°C. These zones represent temperature ranges with the same active chemical reactions. The gasification reaction with the biomass chemical composition in the form of $CH_xO_yN_z$ can be seen in Equation 1.2 [9]:

$$CH_xO_yN_z + m_wH_2O + x_g(O_2 + 3.76N_2) \rightarrow$$

$$x_1CO + x_2H_2 + x_3CO_2 + x_4H_2O + x_5CH_4 + (z/2 + x_g 3.76)N_2 \quad (1.2)$$

Other major exothermic reactions in the gasification process can be seen in Eqns. 1.3 – 1.6 [10]. Equations 1.3 and 1.4, the rate of steam reforming and dry reforming reactions, are dominant at higher temperatures (600-800°C) and increase the production of CO and H_2 while breaking down heavier hydrocarbons such as CH_4 and CO_2.

$$CH_4 + H_2O \rightarrow CO + 3H_2 \quad (1.3)$$

$$CH_4 + 0.5O_2 \rightarrow CO + 2H_2 \quad (1.4)$$

Equations 1.5 and 1.6, the Boudouard and primary water-gas reactions, are endothermic and attribute to the increase of CO and H_2 at higher temperatures such as those tested in this work.

$$CO_2 + C \rightarrow 2CO \quad (1.5)$$

$$H_2O + C \rightarrow CO + H_2 \quad (1.6)$$

From these equations and from previous research it is known that through the pyrolysis process, gases such H_2 and CO are produced in higher compositions at higher temperatures. However, many different aspects affect the products of these processes such as: temperature, equivalence ratio, heating rate, residence time, and fuel type.

1.7 Heating Rate

The effect of the heating rate and the final pyrolysis temperature has been found to drive the composition and relative yield of the produced syngas [2]. It was found that H_2 production from pyrolysis was 20% higher at lower heating rates (~9 K/s) than at a rapid heating rate (~17 K/s) [11]. However modern industrial gasifiers are predicted to have a rapid heating rate (~100 – 500 K/s). The heating rate for this work was determined to be a function of the specific heat (N_2, biomass), mass flow rate (N_2), mass of the biomass and temperature increase [12]. It was estimated for this experiment to be to be ~100 K/s. A heating rate >500 K/s was used by one author, however the particle size and mass of the tested biomass was significantly smaller than those used in this work and therefore it can be estimated that the heating rates would be similar [6]. Numerous works have used low heating rates to find the final composition of the gases but little has been done with rapid heating rates and its effect on the decomposition and gas evolution [11 and 13].

1.8 Simulations

Simulations of the gasification are numerous however most analyze the gasification process as a whole rather than just the pyrolysis stage which lasts for about $1/10^{th}$ of the entire process. Steam gasification has been simulated using ASPEN PLUS

[4] for pine sawdust. Familiar trends such as an increase in hydrogen production and carbon conversion efficiency with an increase in temperature were observed. However, the main focus of the simulation was on the char gasification and oxidation stage of the gasification process and the pyrolysis (which is known to last from 250 – 300 seconds [2]) was assumed to be instantaneous. Another recent simulation simulated steam gasification from 600 - 1200°C using an equilibrium modeling in MATLAB and again, similar trends were seen [9].

Two main models exist for modeling pyrolysis, kinetic and equilibrium. At low reaction temperatures (<800°C) the reaction rate is slower and the chemical reactions do not reach equilibrium [3]. At these low temperatures, kinetic modeling is necessary and this work aims to aid this process. This modeling technique is necessary for moderate operating temperatures often seen in fluidized bed gasifiers. For entrained flow reactors, the reaction rate and operating temperature (> 1200°C) are high and the equilibrium model is applicable. Although repeated trends are being seen across numerous publications, the modeling assumptions yield results that require significant experimental data for validation and model tuning. It is important that more accurate models are produced through experimental data.

1.9 Typical Gas Compositions

Table 1.2 [14] shows the typical gas compositions from gasification gas (GG), pyrolysis gas (PG), landfill gas (LG), and syngas (SG) for numerous materials and reaction agents. For gasification gases, in particular the first four (due to their low nitrogen content similar to the materials tested here), CO, CO_2, and H_2 make up ~ 80 – 90% of the total gasification gas concentration. Also, less than 10% of the gas

concentration is from CH_4. For pyrolysis gases (PG-D, PG-Le, and PG-Lu), high CO and CO_2 concentrations were measured. Significantly lower H_2 concentrations were also measured due to the pyrolysis duration. Pyrolysis is a rapid process followed by char gasification (as discussed in Section 1.1), which is a slow process lasting an order of magnitude longer. During char gasification, heavier hydrocarbons are broken down into their base components, H_2 and C. However, pyrolysis gases never reach char gasification and many of the heavier hydrocarbons remain and low H_2 concentrations can be observed. It can be expected that the permanent gas concentration produced in this work will have similar results to the pyrolysis gases. The work featured in Table 1.2 shows the total gas concentration produced from the entire process (cumulative production), this work will focus on how the gas is produced through pyrolysis (gas evolution).

Table 1.2 - Biomass derived gas compositions [14]

BDGs	CO	CO_2	H_2	CH_4	C_2H_4	N_2	LHV, MJ/kg	Biomass	Reaction agent
GG-H	0.355	0.27	0.287	0.065	0	0.023	9.2	Cellulose	Air–steam
GG-V	0.197	0.06	0.591	0.115	0	0.037	23.7	Crude glycerol	Steam
GG-L1	0.2792	0.3011	0.3539	0.0436	0	0.0222	8.6	Pine wood	Air
GG-L2	0.3765	0.2889	0.2717	0.0478	0	0.0151	8.4	Pine wood	Oxygen/steam
GG-W	0.2	0.12	0.18	0.02	0	0.48	4.6	Wood	Air
GG-C	0.3	0.02	0.07	0.01	0	0.6	4.2	Charcoal	Air
GG-S	0.24	0	0.21	0	0	0.55	5.2	Biomass wastes	Air
GG-Vä	0.19	0.132	0.12	0.058	0	0.5	4.9	Wood	Air
PG-D	0.568	0.042	0.216	0.102	0.051	0.021	15.8	Sylvester pine and spruce	–
PG-Le	0.511	0.258	0.087	0.083	0.025	0.036	8.8	Pressed oak and beech sawdusts	–
PG-Lu	0.26	0.615	0.016	0.083	0	0.026	3.9	Pine bark	–
LG-B	0	0.5	0	0.5	0	0	13.3	Organic wastes	Bacteria
LG-R1	0	0.41	0	0.53	0	0.06	15.0	Organic wastes	
LG-R2	0	0.037	0	0.9	0	0.063	40.5	Organic wastes	Water wash
Methane	0	0	0	1	0	0	50.0	–	–
SG-50	0.5	0	0.5	0	0	0	17.4	–	–
SG-5	0.95	0	0.05	0	0	0	10.5	–	–

1.10 Previous Biomass Gasification Research at The University of Iowa

The biomass gasification project was started by Kevin O'Donnel to coincide with The University of Iowa's partnership with Quaker Oats [16]. The first version of the

gasifier was designed by Kevin and the current industrial heater was purchased. Andre Lenert built upon Kevin's setup and explored the evolution of H_2, CO, and nitric oxide (NO) from gasification of oat hulls. Experiments were conducted for low temperatures ranging between 300 - 500°C. Lenert found that oat hull pyrolysis was rapid at low temperatures. Also, the yield of H_2 and CO was found to be proportional to the yield of the environmentally harmful NO. Additional studies conducted by Lenert focused on adapting the pyrolysis results for wood shavings into useful equations that could later be applied to CFD models [16].

Eric DeCristofaro took over the gasification research in the Fall of 2008 and focused on expanding the temperature range as well as increasing the number of measurable gases. Typical gasification temperatures range from 600 - 1000°C, however, Lenert's work focused on low temperature gasification (300 - 500°C). DeCristofaro added an O_2 and CH_4 torch to setup to raise the temperature range to 400 - 800°C. This range represents a more applicable temperature range that is more easily compared to other experimental and simulated results [16]. The current experimental setup uses the same heating method (O_2/CH_4 torch in conjunction with the industrial heater) however numerous minute changes were made to increase the repeatability of the experiment. During experimentation, the torch would frequently extinguish itself during tests, working less than 20% of the time. Pressure changes and torch instabilities were main causes of the extinguishing flame and were addressed in the current setup.

Sensors from DeCristofaro's research were less effective than planned. The sensors used in the experiment included: H_2, CO, CO_2, CH_4, CO_2, O_2, and a joint temperature/humidity sensor. However, useful data was only gathered on the H_2, O_2, CO and CO_2 sensors. The CO and CO_2 results showed the gas evolution throughout the

pyrolysis while the H_2 was not sensitive enough to detect H_2 concentration changes. Also, the O_2 sensor was only used to measure the equivalence ratio and the evolution of the O_2 from pyrolysis was ignored. Data from the CH_4 sensor and the temperature/humidity sensor was never used.

DeCristofaro's results showed that increases in temperature were found to be inversely proportional to the pyrolysis duration and proportional to CO production, as expected, while CO_2 production was found to be insensitive to changes in temperature. Equations were created that accurately described the CO and CO_2 production as well as the total gas yield. The effect of equivalence ratio was examined at 700℃ for O_2 concentrations between 0 – 20.95%. At 10% O_2, CO and CO_2 production was at its highest however pyrolysis occurred fastest at 20.95% where air was directly combusted with the biomass. CO production at 10% O_2 was ~300% higher than with 0% O_2 as expected. CO_2 production however, was again ~300% higher at 20.95% O_2 than at 0%.

This work focuses on expanding DeCristofaro's work in three main areas:

1. Increasing the efficiency and repeatability of the experimental setup
2. Increasing the measurable gases
3. Expanding the analysis of the results

By focusing on these three areas, the goal was to make this research more useful to other researchers and engineers.

CHAPTER 2

MATERIALS AND TESTING METHODS

2.1 Materials

Three materials including corn, paper sludge, and oat hulls have been explored in this work for their local abundance and low cost. Corn, already used as a renewable energy source in the form of ethanol, is locally abundant most places in Iowa. Every year thousands of bushels of treated seed corn is wasted or goes unused. This waste is considered toxic and is required by law to be stored 18 inches under the soil in an isolated area far from water supplies [15]. The corn's toxicity is associated with the pesticides and fungicides applied to the corn before it is planted. If the toxic additives could be removed through high temperature gasification with a long solid residence time, the treated seed corn could be used as a fuel source in biomass power plants. However, the insecticides used in common treated seed corn is known to produce toxic gases if exposed to high temperatures and is allowed to decompose. Before the use of treated seed corn in biomass facilities is feasible, extensive research on methods to avoid toxic decomposition is needed. Still, untreated seed corn and corn stover are abundant and available in Iowa as a biomass source.

The paper sludge is from a company in Cedar Rapids, Iowa called Weyerhaeuser. The pulp is the result of recycling cardboard and creating new cardboard pallets. The parts that can no longer be recycled or are left after the creating process are known as paper sludge. It contains small strands of paper, sand, and a very small plastic contaminant. They create around 62,000 wet tons per year at around 50% moisture content.

The motivation to study oat hulls came from the success of a joint project between the University of Iowa and Quaker Oats to co-fire oat hulls (with coal) in the University's Stoker boiler, saving money and reducing undesirable emissions [1]. The oat hulls were purchased from Quaker Oats for a fraction of the cost of coal. Over 160 tons of oat hulls are delivered to the University by Quaker Oats each day which reduces Quaker Oats' costly waste disposal fees and Iowa landfill space. The oat hulls are not processed before co-firing in the Stoker Boiler.

The ultimate and proximate analysis of the materials can be seen in Table 2.1 and Table 2.2. This knowledge allows one to predict the volatile products produced through gasification. If higher percentages of C exist, then CO and CO_2 production will likely be higher. From the ultimate and proximate analysis we can predict that the majority of the permanent gases produced through pyrolysis will be composed of mostly CO and CO_2 due to the high C and O present within the material. Also, low hydrogen concentrations can be expected due to little hydrogen in the makeup of the three materials as well as the experimental focus on pyrolysis (see Section 1.9)

Table 2.1: Material Ultimate Analysis

	Seed Corn	Paper Sludge	Oat Hulls
Moisture	11.59%	46.99%	10.43%
Carbon	39.13%	22.97%	43.51%
Hydrogen	5.50%	2.88%	4.71%
Nitrogen	1.28%	0.05%	0.65%
Chlorine	0.04%	0.01%	0.15%
Sulfur	0.10%	0.07%	0.04%
Ash	0.83%	7.03%	5.22%
Oxygen	41.53%	20%	35.44%
Total	100%	100%	100%

Table 2.2: Material Proximate Analysis

	Seed Corn	Paper Sludge	Oat Hulls
Moisture	12.91%	46.99%	10.43%
Volatile Matter	74.42%	44.99%	67.80%
Fixed Carbon	7.46%	0.99%	16.55%
Ash	5.21%	7.03%	5.22%
Total	100.00%	100.00%	100.00%
HV [BTU/lb]	8,910	3,556	6,934

2.2 Experimental Setup

The experimental setup used in this work is similar to and was built upon DeCristofaro's and Lenert's work. Numerous modifications have been made to their setups and are discussed later. The setup, as seen in Figure 2.1 and 2.2, shows the main components of the system used to gasify the materials. Figure 2.1 is a schematic of the system and shows most of the main components including the industrial heater, torch systems, thermocouples, flow controllers, and the spark ignition system. Figure 2.2 shows the setup as is during July 2010 experiments. Notables not seen in the schematic include the particulate filters, sensor bank, power supplies, and the actual working environment. A full list of the components used in the experiment can be seen in Table 2.3.

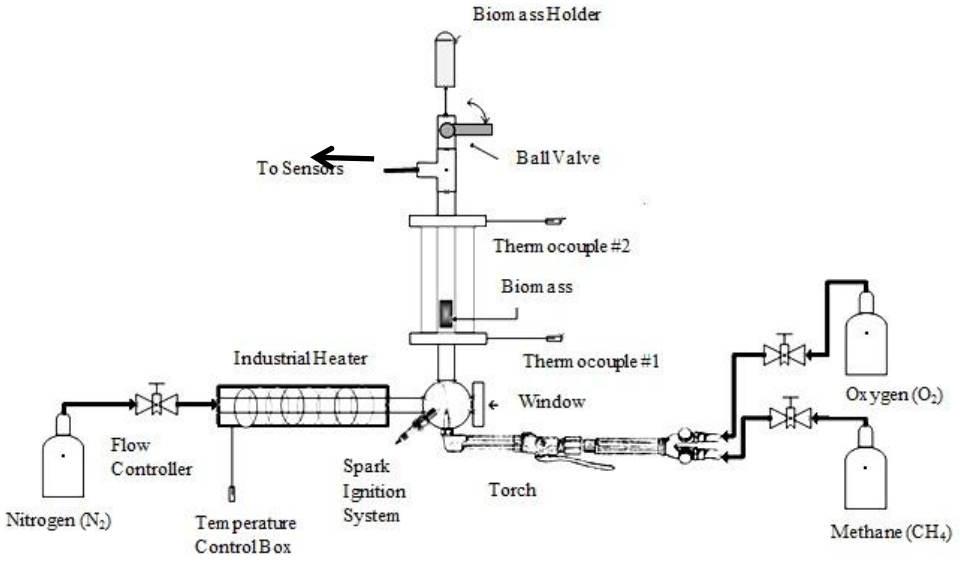

Figure 2.1: Schematic of experimental setup

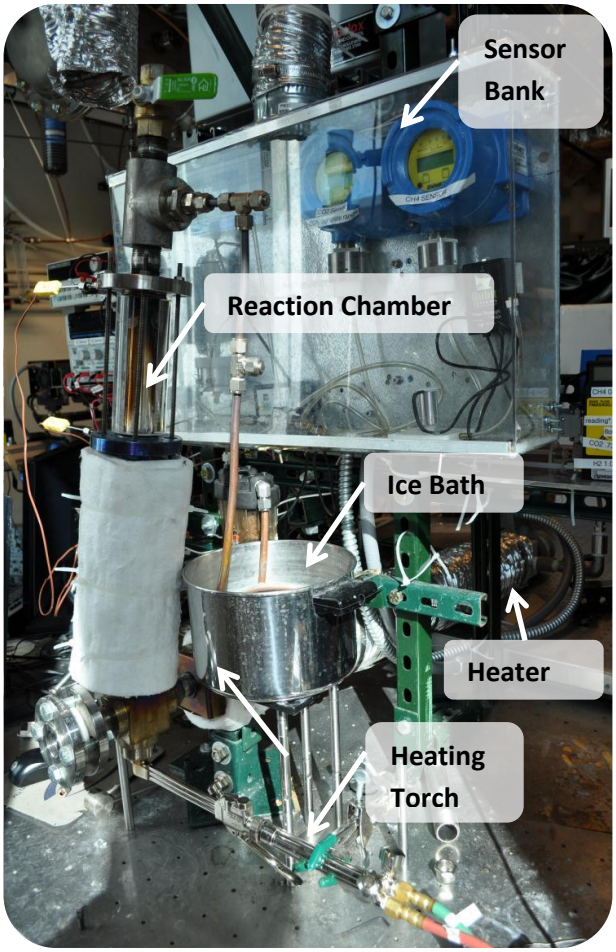

Figure 2.2: Actual experimental setup

Figure 2.3 shows a complex flow chart of the setup and a majority of its components including the sensors, computer, gas tanks, and power supplies.

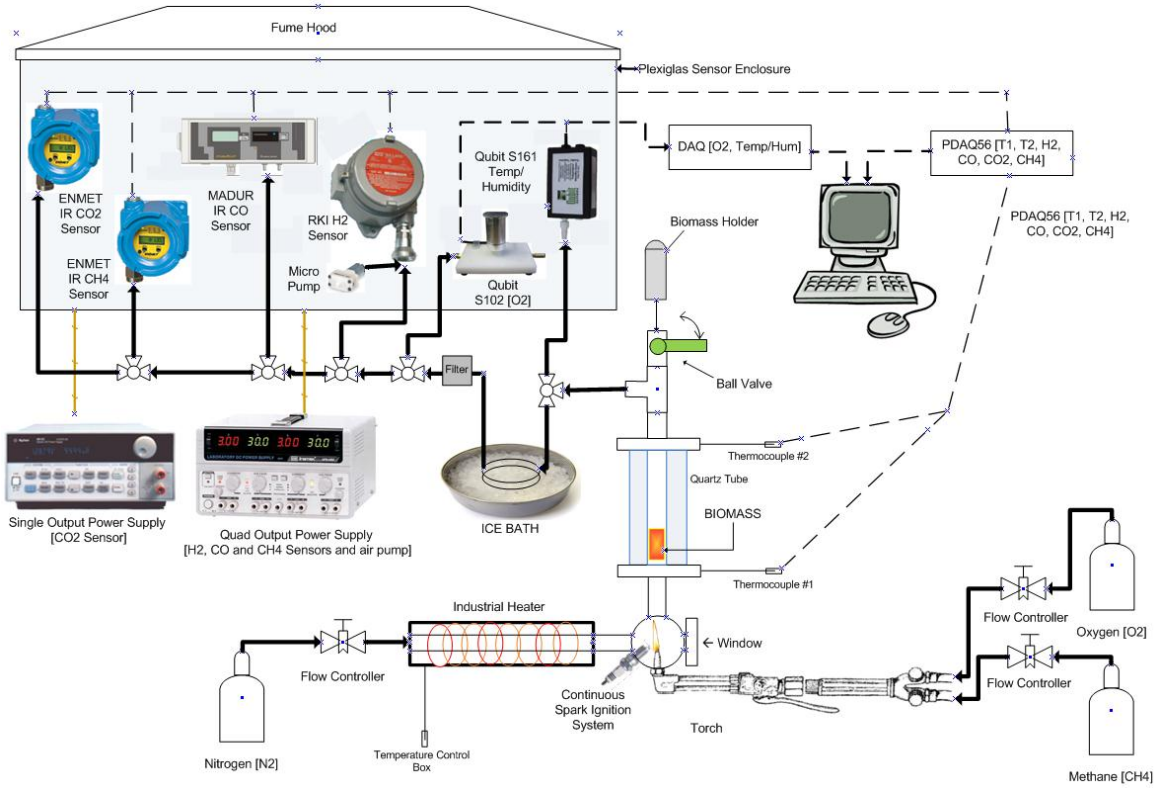

Figure 2.3: Experimental setup and flow chart

Table 2.3: Experiment components

Equipment List	
250 Ω resistors (4)	Micro air pump
Biomass Injection Valve	Nitrogen Tank
Biomass Samples	Omega FMA-5400 Flow Controller
Chromalox Industrial Heater	Omega FMA-A2409 Flow Controller
Computer with DASYLab	Oxy-acetylene torch
Data Acquisition Card (2)	Oxygen Tank
DC Power Source w/ connection cables (2)	Particle/moisture Filter (2)
Exhaust fan	Lexan enclosure
H2 Sensor	Quartz tube
High Precision Scale	Qubit Systems Oxygen Sensor
High temperature insulation	Qubit Temperature/Humidity sensor
Ice bath	Rotameter
IR CH4 Sensor	Screen Packet
IR CO Sensor	Stainless steel mesh
IR CO2 Sensor	Tubing and fittings
Lighter	Type K thermocouples (2)

2.2.1 Sensors

To detect the instantaneous gas release from pyrolysis of the biomass, sensors connected in parallel were used. Calibration techniques from DeCristofaro were followed [16] and the sensor bank remained largely unchanged. Notable additions to the sensors include working CH_4 and O_2 sensors. In DeCristofaro's work, only the CO and CO_2 sensor data was collected even though the other sensors were in place. Also, the O_2 sensor was only used to measure the equivalence ratio and the CH_4 sensor was never properly implemented. This work continues to collect CO and CO_2 concentrations, as well as instantaneous CH_4 and O_2 concentrations. H_2 data was collected in both works; however, numerous design issues prevented measurable concentrations and is discussed later (Section 3.5). A humidity/temperature sensor was employed; however, the particulate filters used to filter the tar also remove large amounts of moisture, resulting in

inaccurate humidity readings. Table 2.4 shows the sensors used in this work and their properties. Data collected from the sensors is sent through a data acquisition card to personal computer and is managed and recorded through DASYLab.

Table 2.4: Sensor information

Gas	Description	Type	Range	Relative Accuracy
H_2	RKI Instruments S-Series LEL	Catalytic Combustion	0-5800 ppm	6.43%
CO	ENMET MadIR-DO1	IR	0-10% by vol	5.35%
CH_4	ENMET EX-5120	IR	0-5% by vol	5.76%
CO_2	ENMET EX-5165	IR	1.5-20% by vol	2.1%
O_2	Qubit S102	Electrochemical	0-30% by vol	±0.0525%
Humidity	Qubit S161	Capacitive Element	100%	±1.0%
Temp	Qubit S161	Band Gap Principal	-50 to 100 C	$< \pm 1^{o}C$

2.2.2 Joint Heating System

The heating system employed for this experiment is a joint heating system using both an industrial electric heater and a heating torch. The industrial heater, a horizontal Chromalox 9kW GCHMTI flow heater with a stainless steel body and three INCOLOY sheath elements, was used to preheat the N_2 to ~300 - 400°C. The heated flow then passes over the O2/CH4 torch and the resulting flow is heated to temperatures between 400 - 800°C, the pyrolysis temperature of the experiment. See Figure 2.4 for a diagram of the joint heating system.

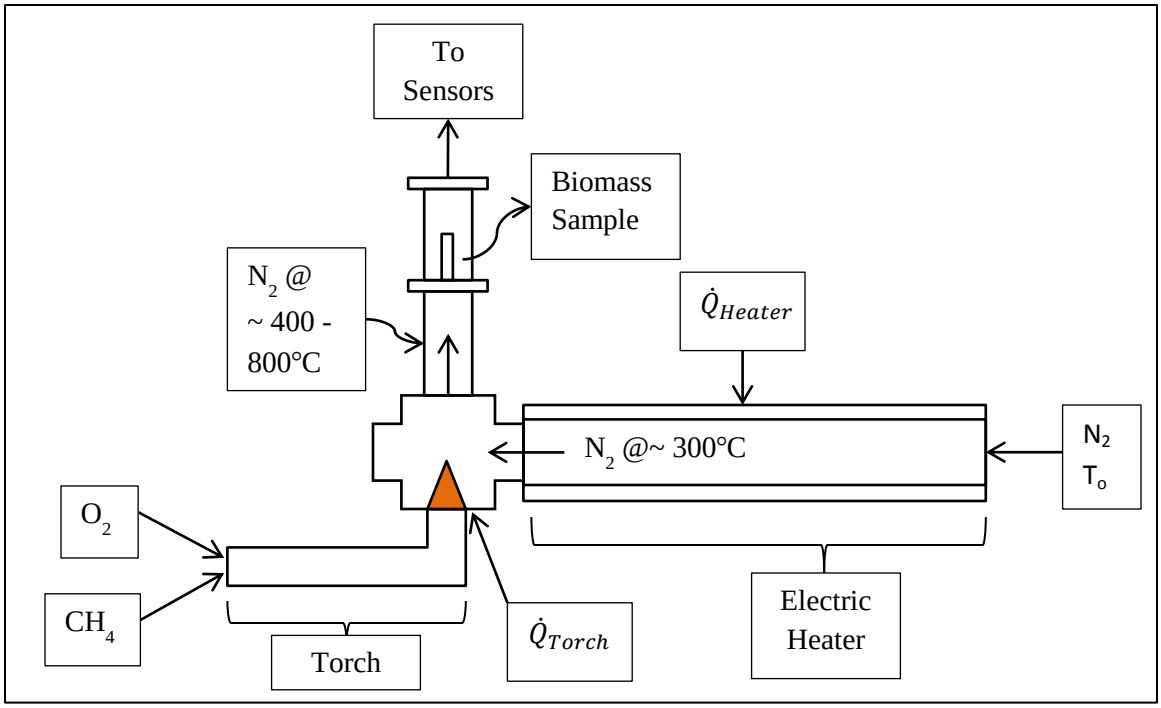

Figure 2.4: Electric heater/torch diagram

As stated earlier, the previous version of this setup experienced difficulty with the torch. The torch would frequently extinguish itself during experiments. When the sample is dropped into the reaction chamber, a pressure change would occur and extinguish the flame. The flame would also go out in between experiments and when the char was removed. It was first believed that the torch tip was over heating and this caused the flame to become unstable. To counteract this, DeCristofaro cooled the torch with ice during experiments. This method did increase the flame stability slightly and he was able to complete his work; however, the flame still frequently extinguished itself during experiments.

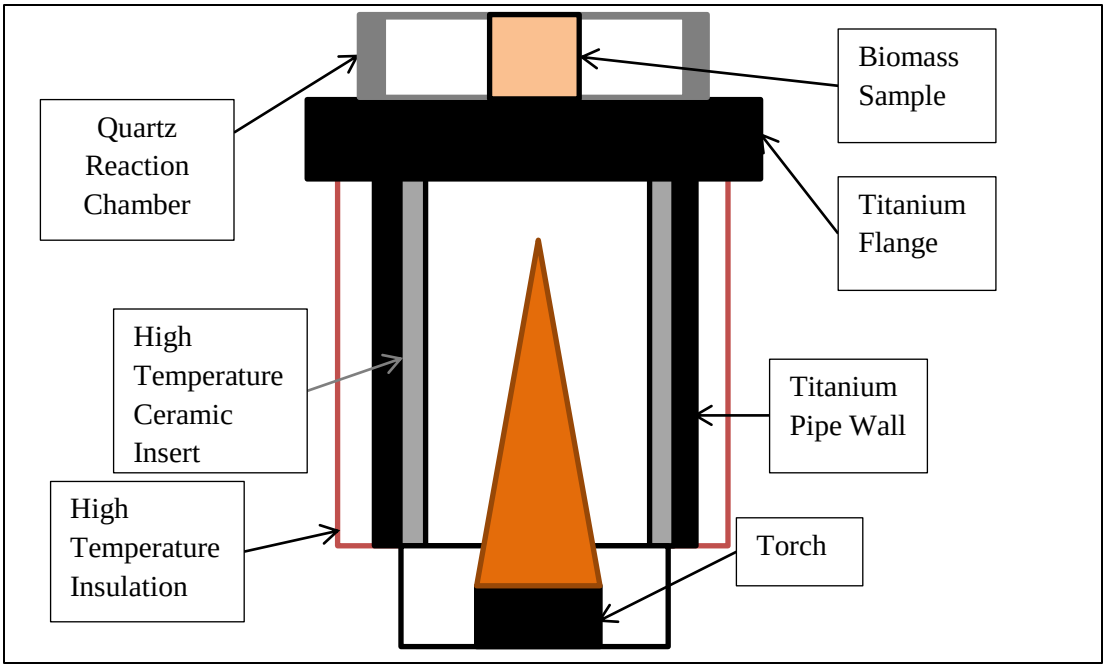

Figure 2.5: Insulation and titanium pipe/flange diagram

This work attempted to increase the reliability of the torch. When experiments for this work were first started in the Fall of 2009, similar torch issues existed. Numerous changes were made to counteract this instability. First, the setup was poorly insulated and was losing large amounts of heat. To counteract this, new insulation was added outside and inside the pipe walls of the setup. High temperature insulation was wrapped around the outside of the pipe wall as seen in Figure 2.5. Inside of the pipe, a high temperature ceramic was inserted. The hope was that if the inside of the pipe maintained its heat, then the flame would not bounce off of cold walls, increasing the instability of the flame. The next addition was the use of titanium pipes and flanges. The titanium can withstand high temperatures and has a lower specific heat. This addition again helped the experiment maintain the heat produced from the torch and electric heater. The third and most important change was a new torch tip, specifically designed for natural gas and O_2.

The tip used in DeCristofaro's work was designed for acetylene and O_2 and acetylene burns quicker than CH_4 and natural gas. These three additions significantly increased the reliability of the torch and it never extinguished itself during any of the experiments used for the results of this work.

2.3 Procedure

The procedure for this experiment is in place to ensure that the data gathered is repeatable and that, more importantly, safety standards are maintained. A non-descriptive list of steps followed before, during, and after experimentation is shown below:

1. Turn on exhaust system
2. Check gas lines
3. Turn on sensors/flow meters
4. Prepare ice bath
5. Turn on compressed air
6. Turn on electric heater – set temperature
7. Open DASYLab experiment file
8. Prepare test samples during heating
9. Turn on O_2/CH_4 lines
10. Light and insert torch once desired electric heater temperature is reached
11. Adjust O_2/CH_4 flow rates with temperature
12. Once experimental temperature is reached, turn OFF air, turn ON N_2
13. Set N_2 flow rate to 23.7 L/min
14. Perform experiments
15. Perform cool down procedure
16. Analyze data

A day before experimentation, the sensors are calibrated and the system is cleaned. On the day of experimentation, the first step is to turn the exhaust system *on*. This exhaust system increases the airflow out of the room and only allows gas from the gas tanks (O_2, CH_4, and N_2) to flow to the setup if the system is turned on. A few minutes will pass while the system turns on and during this time gas lines should be

traced from the tank to the setup to ensure that everything is configured correctly. Flow meters to the O_2 and CH_4 lines should then be turned on along with the sensors. To turn on the sensors, the two power supplies must first be turned on and then appropriate voltages must be applied to the individual sensors based on their channel. An INSTEK quad output power supply and an Agilent power supply are used to power the sensors and the appropriate voltages can be seen by channel number in Table 2.5.

Table 2.5: Power supply voltages

Source	Voltage [V]
INSTEK Channel 1	24
INSTEK Channel 2	24
INSTEK Channel 3	3
INSTEK Channel 4	15
Agilent Main Channel	20

After the sensors are on, an ice bath should be prepared. The ice bath cools the gasification gas before it enters the sensors to prevent damage to the sensors. Next the compressed air and electric heater are turned on sequentially. Compressed air is used to preheat the system rather than nitrogen because it is not bottled. The air comes from a compressor on the roof of the Seaman's Center while the N_2 is bottled and more expensive. The heater temperature is then set according to the desired experimental temperature. Generally, if higher experimental temperatures are desired such as 800℃, then the heater is set to a maximum of 400℃, whereas if lower temperatures such as 500 - 600℃, then the heater is set to 200 - 300℃. The compressed air must be flowing

through the electric heater *before* it is turned on to ensure that the INCOLOY elements, used to heat the fluid, to not overheat and melt.

Once the heater is set, DASYLab and Logger Pro files designed for the experiment are opened. The DASYLab file shows the temperature output and the gas concentrations for: CO, CO_2, CH_4, and H_2 while Logger Pro is used to measure the concentration of O_2. The files are opened at this time to monitor the temperature across the reaction chamber. Preheating with the electric heater takes time and during the wait samples are prepared into sample packets. Steel mesh is bent into a cylindrical shape to form the packets and biomass at 0.5 grams is inserted. The packets are reusable and are removed from the experiment after the sample is gathered.

Once the system reaches the temperature set on the electric heater, the O_2 and CH_4 bottles are turned on and the flow rates are set according to the desired temperature. The ratio between the flow rate of O_2 and CH_4 is held constant at 2.64 (Q_{O2}/Q_{CH4}) to ensure any excess O_2 not burned through combustion is known and can be accounted for within the results. Next the torch is lit using a grill lighter and the nozzles are slowly opened until a stable flame is produced. The torch is then inserted into the setup and is screwed in place using a custom set screw which applies pressure to the torch, keeping it secure. The temperature is then monitored as the experiment heats up to the desired chamber temperature. Setting the flow rates to reach this desired temperature is a trial and error process where previous known flow rates are first used that produced a certain temperature are attempted and then the flow rate are increase or lowered until the desired temperature is obtained.

When the desired chamber temperature is reached, the compressed air valve can be turned to *off* and the N_2 bottle can be opened and the N_2 flow rate is set at 23.7 L/min.

This flow rate was set to increase the heating rate to mimic an industrial gasification system while also protecting the electric heating elements from overheating. During the change of the gasifying agent (air to N_2), the torch should be monitored at all times. With the *previous setup* by DeCristofaro, during this change in gasifying agent the torch would become unstable and extinguish itself, releasing O_2 and CH_4 gas into the experiment and surroundings. A large exhaust fan was turned on in this case as a safety precaution on top of the exhaust system already in place. With the *current setup*, however, torch stability is much less of an issue and the torch rarely extinguishes itself. Even so, the torch is still monitored as a safety precaution.

Within a few minutes of the gasifying agent switch, the experiment will reach equilibrium and testing can begin. The exact time (H:M:S), material, O_2/CH_4 flow rates, starting chamber temperature, and heater set point temperature are recorded prior to dropping the sample. The sample is dropped by inserting the packet into the biomass holder which is a pipe that is sealed on one side that screws onto the top of a ball valve. This holder lowers the pressure drop within the system during the sample insertion. This pressure drop can extinguish the flame and was a large issue with previous experiments. The ball valve is then opened and the sample will drop into the reaction chamber. The ball valve is then closed to redirect the gasification gas into the ice bath and sensors. The sample stays within the chamber for 3 minutes and is then removed. The experiment is then allowed a few minutes to reach equilibrium and information is again recorded before another sample is dropped. Five samples are averaged for each material at a certain temperature. The temperature range is examined from 400 - 800℃ and samples were taken in approximately 100℃ intervals. Table 2.6 shows a summary of the experimental parameters used.

Table 2.6: Experimental parameter summary

Parameter	**Setting**
O_2/CH_4 Ratio	2.64
N_2 Flow Rate	23.7 L/min
Solid Residence Time	3 minutes
Chamber Temperature Range	400 - 800℃
Sensors	CO, CO_2, CH_4, H_2, O_2
Samples Conducted Per Material and Temperature	5
Sample Mass	0.5 grams

Once the experiment is complete, the N_2, CH_4, and O_2 bottles are turned *off* and the compressed air valve is turned to *on*. The electric heater and torch are both turned *off* as well. The flow rate of compressed air is set to its maximum value to increase the air cooling of the system. The torch is removed and is relit outside of the experiment to drain excess gas in the O_2 and CH_4 lines. The ball valve used to drop the sample packets is set to direct the flow out of the experiment, directly into the exhaust rather than through the sensors. The data gathered in DASYLab and Logger Pro is imported into Microsoft Excel 2010 where analysis is conducted. The sensors may also be turned off once the data is imported into Excel. Once the system has reached a cool temperature (< 80℃) and the excess gas is burned off, the system can be shut off.

CHAPTER 3

RESULTS AND DISCUSSION

3.1 Excess Oxygen Volumes

Equivalence ratio plays a vital role in the production of CO [16] and it is known that gasification rarely occurs without O_2 present. To maximize CO production in the pyrolysis gas, a concentration of excess O_2 is added to the gasification agent (N_2) based on the ratio of the heating torch's flow rates. The excess O_2 concentration is introduced through the torch and is un-combusted O_2 that did not react with CH_4 used to heat the N_2 stream. The ratio found to maximize the CO production was determined experimentally and is 2.64 LPM of O_2 for each LPM of CH_4. The flow rates were determined by two variables, first the ratio of O_2 to CH_4 and second the amount of heat needed to maintain each temperature range. Higher flow rates are used for higher temperatures and resulted in higher excess O_2 volumes due to dilution from the large flow rate of N_2. To determine the excess O_2 volume, a stoichiometric balance on the torch was used as seen in Equation 3.1:

$$xCH_4 + yO_2 + zN_2 \rightarrow aCO_2 + bH_2O + cN_2 + dO_2(0.64) \quad (3.1)$$

Solving for *a*, *b*, *c*, and *d* from the known values (*x*, *y*, and *z*) and finding *d* as a percentage of the total pyrolysis gas volume we can find the excess O_2 volume. Table 3.1 shows the excess O_2 volume for each material and temperature range.

Table 3.1: Excess O_2 volume per temperature range and material

	Corn	Crushed Corn	Oat Hulls	Paper Sludge
~ 800°C	7.508 %	7.508 %	7.623 %	7.508 %
~ 700°C	6.982 %	6.411 %	6.165 %	6.258 %
~ 600°C	5.594 %	5.561 %	5.116 %	5.561 %
~ 500°C	5.028 %	4.579 %	4.940 %	5.513 %
~ 400°C	4.003 %	4.361 %	4.000 %	4.361 %

The values seen in Table 3.2 change with temperature due to the higher flow rates needed to maintain higher temperatures. As the temperature decreases along with the torch flow rates, the O_2 concentration becomes more diluted than it was at higher temperatures. Table 3.2 shows the excess O_2 volumes from the torch, undiluted by the constant N_2 flow rate of 23.7 LPM. The excess O_2 volume from the torch is fairly constant at about 29 – 30%. The reason the values are not equal is due to difficulty in setting a specific flow rate in the flow meters. The ratio of O_2 to CH_4 flow rates used was determined experimentally to minimize the CO production in torch combustion and maximize the CO gasification yields. Excess O_2 concentrations seen in Table 3.2 are only for oat hulls; however, since the ratio of O_2 to CH_4 is nearly constant throughout the results, the O_2 concentrations for other materials are similar.

Table 3.2: Undiluted excess O_2 concentrations from the torch for oat hulls

Temperature	O_2 Flow Rate (LPM)	CH_4 Flow Rate (LPM)	Excess O_2 from Torch	O_2/CH_4 Ratio
791℃	5.03	1.908	29.78%	2.636
686℃	3.79	1.435	29.94%	2.641
592℃	3.24	1.250	29.30%	2.592
515℃	2.86	1.080	30.17%	2.648
400℃	2.21	0.861	27.42%	2.567

3.2 Carbon Monoxide Evolution & Production

To determine the mass of CO produced throughout pyrolysis as well as the final yield, Equations 3.2 & 3.3 are used [16]. Equation 3.2 determines the gas evolution while Equation 3.3 calculates the cumulative mass produced throughout the pyrolysis where ΔT is 1 second, Q is the nitrogen flow rate [L/s], γ_{gas} is the concentration of the target gas, R is the universal gas constant [L-atm/mol-k], P_{atm} is atmospheric pressure [atm], M_w is the molar weight of the target gas [g/mol], and T_{amb} is the ambient temperature [K].

$$m(t) = \frac{M_W \gamma_{gas} P_{atm} Q \Delta T}{R T_{amb}} \tag{3.2}$$

$$m(t) = \sum_0^{n=t} \frac{M_W \gamma_{gas} P_{atm} Q \Delta T}{R T_{amb}} \tag{3.3}$$

Using these calculations, the mass of CO and CO_2 was determined from the gas concentrations measured in the experiment. The gas evolution for CO can be seen for all of the tested materials in Figure 3.1. Each data series represents the average of 5 repetitions for each material at each temperature at ~ 800℃, 700℃, 600℃, 500℃, and

400℃. The temperatures listed in the plot are the average bed temperature throughout the solid residence time.

For all the materials tested, the pyrolysis temperature is generally inversely proportional to the pyrolysis duration. The pyrolysis duration is where the majority of the volatiles are released and ends when gas evolution is negligible. Table 3.3 shows the approximate pyrolysis duration (identified as when the slope of the data series reaches ~0) for the materials at each temperature series. From this table, it can be seen that oat hulls have the shortest pyrolysis times. For the other materials (corn kernels, crush corn, and paper sludge), the pyrolysis occurs significantly slower as the temperature decreases with the exception of corn kernels at 600℃ which occurs faster than at 700℃. This could be due to the size of the corn kernel and the surface area it has exposed to the gasification agent (N_2). The decrease in surface area directly exposed may change how it decomposes and its reaction rate. Also, for the oat hulls, it can be seen that peak production of CO occurs at nearly the same time for each temperature series. For the other materials, as the temperature decreases, peak production time increases. Again, this could be due to the density and surface area of the oat hulls in comparison to the other materials.

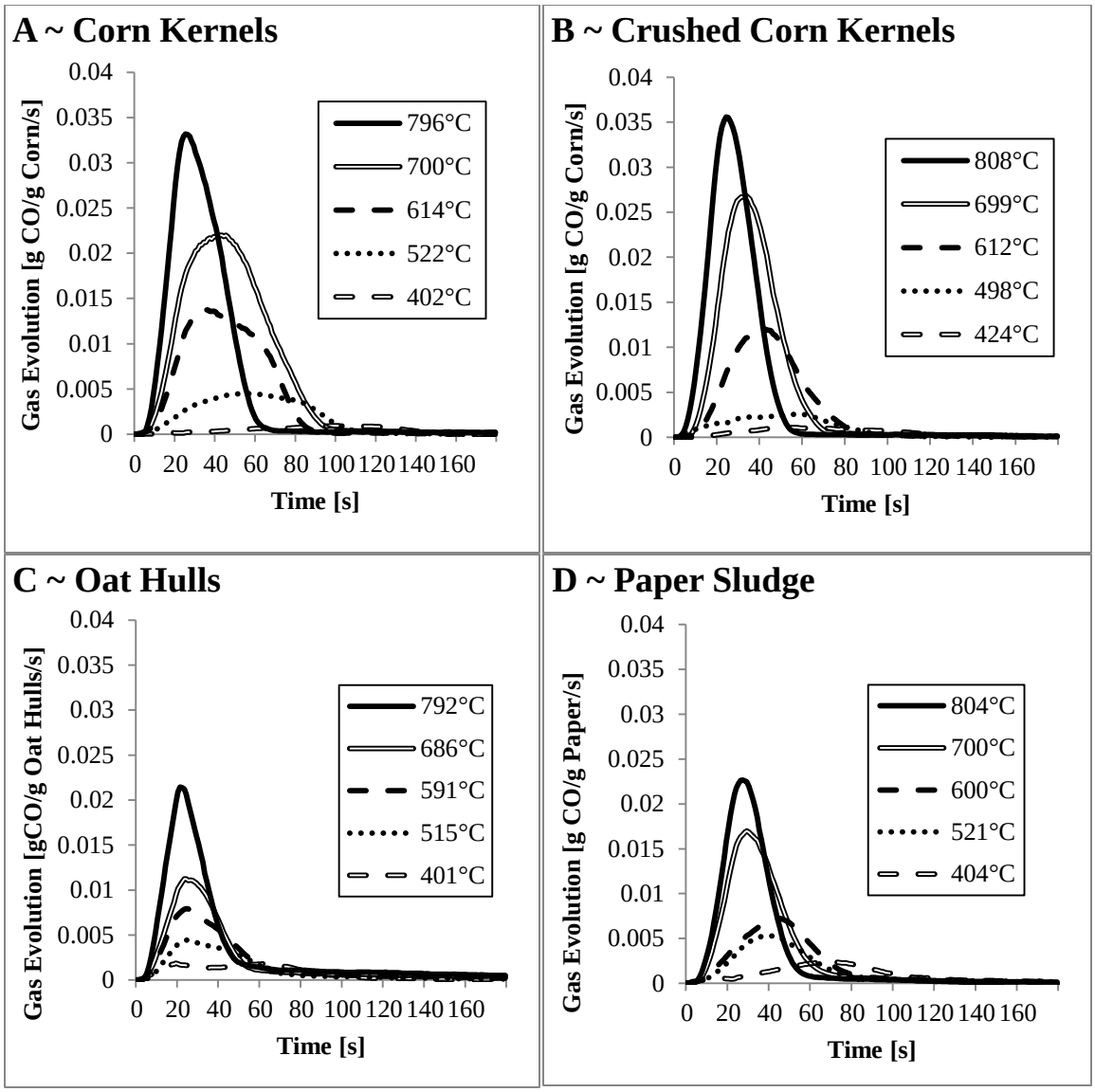

Figure 3.1: CO gas evolution versus time for A) corn kernels, B) crush corn kernels, C) oat hulls, and D) paper sludge

Table 3.3: Approximate pyrolysis duration (in seconds) by material and temperature series

	Corn	Crush Corn	Oat Hulls	Paper Sludge
~800°C	60	52	46	55
~700°C	91	67	55	65
~600°C	80	80	65	71
~500°C	99	82	65	72
~400°C	131	104	80	98

In Figure 3.1 it evident that the peak CO production is much higher for corn and crush corn kernels than it is for oat hulls and paper sludge. This shows that the higher energy density in corn results in greater CO production. To determine the total CO yield, each temperature series was integrated to find the total CO production throughout the pyrolysis process and are plotted in Figure 3.2. Surprisingly, the highest CO yield was produced by whole corn kernels at 700℃. For all other materials, higher temperatures yield higher results; however, for corn kernels this is true except for the temperature series at 700℃ and 796℃. This anomaly could be again related to the surface area exposed to the heated N_2 which is much lower than the other materials (including crushed corn kernels). The crushed corn kernels are composed of small pieces of corn which expose more of the corn to the N_2. The high density and low surface area of corn, along with its inherent chemical makeup, may differentiate the CO yield in comparison to other materials.

Aside from the maximum yield across the materials, CO yields were highest for crushed and whole corn kernels and lowest in oat hulls and paper sludge. For each material, except corn, temperature and CO gas yield were positively related. For oat hulls and corn kernels, the results after the gas production slope decreases were removed to decrease clutter in the figure.

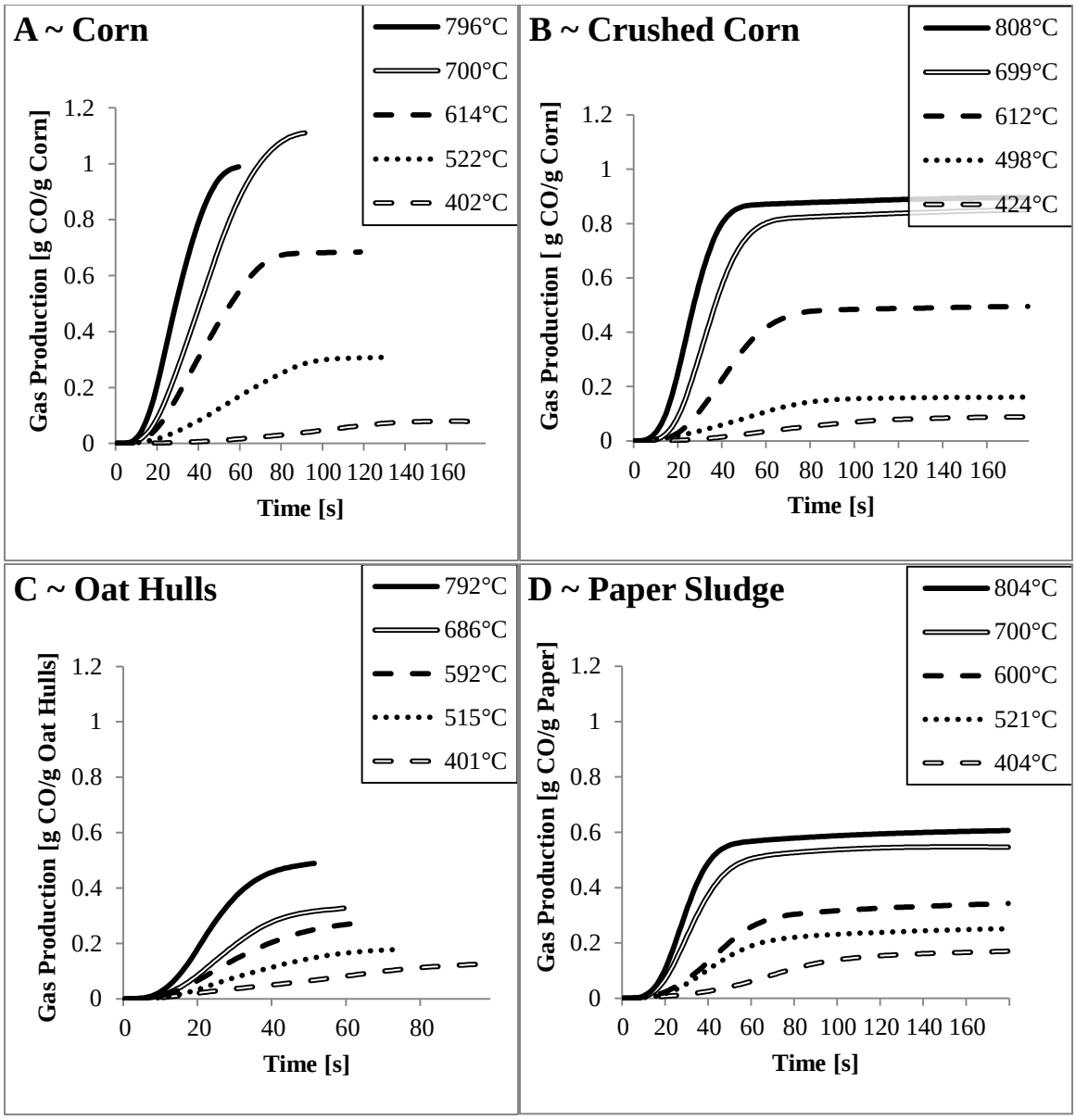

Figure 3.2: CO gas production versus time for A) corn kernels, B) crush corn kernels, C) oat hulls, and D) paper sludge

3.3 Carbon Dioxide Evolution & Production

The CO_2 gas evolution and production were determined in the same method used for the CO, using Equations 3.2 and 3.3. Figure 3.3 shows the CO_2 gas evolution for all four of the materials tested. As seen in the figure, the production of CO_2 is independent of temperature and no particular pattern is consistent for all materials from the gathered

data. The randomness of the results is likely related to the high noise levels produced by the torch. At higher temperatures, CO_2 production from the torch can be as high as 150,000 ppm or 15% of total volume of the pyrolysis gas. The maximum measurable value by the CO_2 sensor is 200,000 ppm or 20% of the income stream. The CO_2 produced from pyrolysis of the biomass is much smaller than the volume produced by the torch (< 1% of the total volume) which can be lost or severely altered by the torch noise.

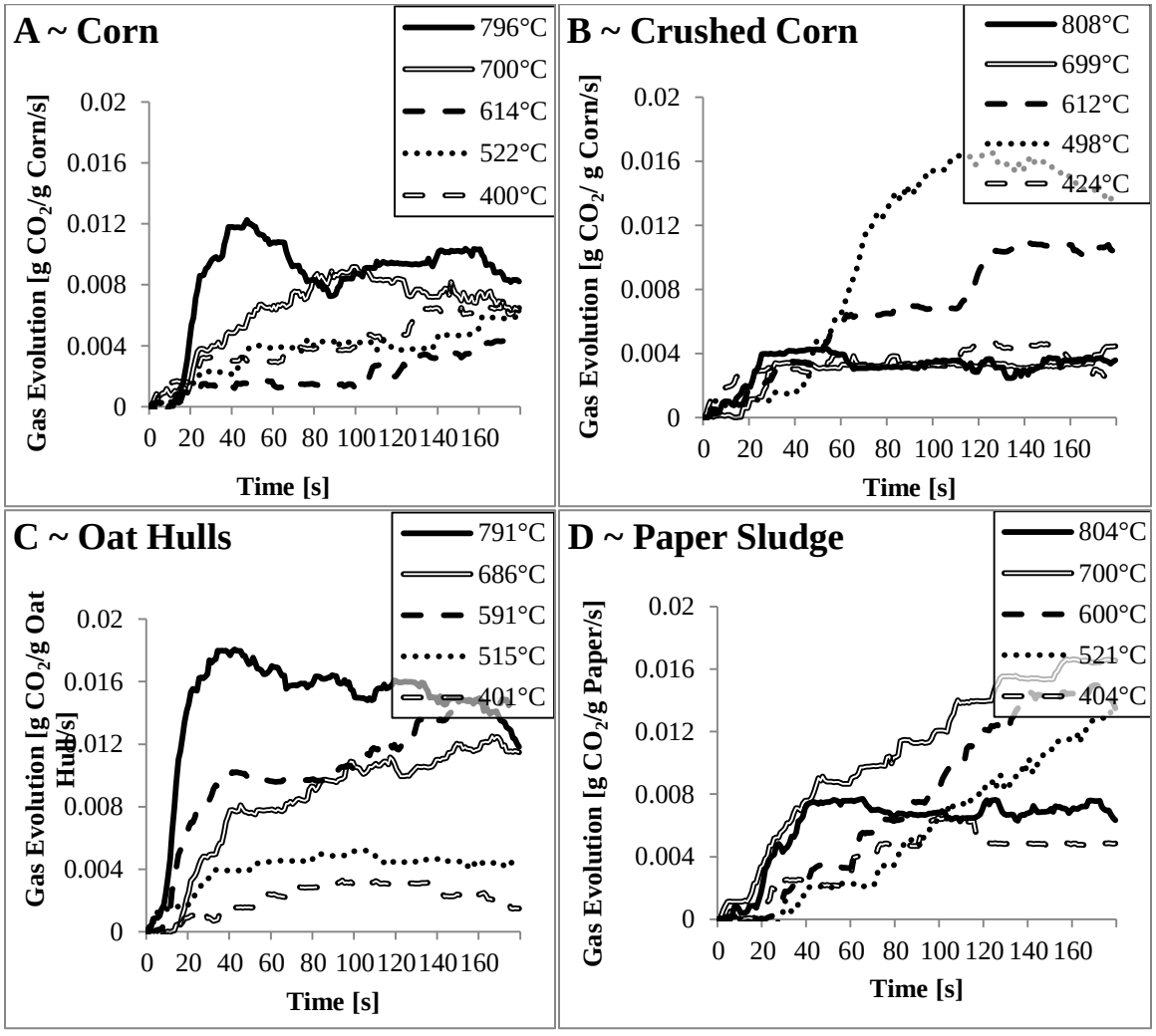

Figure 3.3: CO_2 gas evolution versus time for A) corn kernels, B) crush corn kernels, C) oat hulls, and D) paper sludge

Figure 3.4 shows the cumulative CO_2 produced versus time and it can be seen that the CO_2 production is temperature independent and the slope is mostly constant. The almost constant slopes for all four materials can be attributed to the numerous reactions occurring in the entire gasification and pyrolysis processes. After the initial pyrolysis, reactions occur from tar cracking and char gasification where CO_2 is continually produced. The other permanent gases produced through tar cracking and char gasification are negligible in comparison to the CO_2. Again, the high noise levels in the torch emphasize the randomness seen in the data and provide fairly inconclusive results with a high level of uncertainty. Future work should take action to improve the CO_2 measurements.

3.4 Oxygen Concentrations throughout Pyrolysis

As discussed earlier, O_2 concentrations exist within the heated N_2 stream which significantly affects pyrolysis gas yields. The excess O_2 reacts with the biomass during its decomposition, mixing with C and H_2 to create CO, CO_2, and H_2O. These compounds can again be broken down through heating into their base elements to produce O_2 stored within the biomass. Figure 3.5 shows the evolution of O_2 throughout pyrolysis. In the figure, the O_2 concentration is based on the flow rates of O_2 and CH_4 through the torch (shown in Table 3.1) is subtracted from the measured concentrations to show O_2 production (positive concentrations) and O_2 depletion from reactions with the biomass (negative concentrations). At the initial value of 0% O_2 for all cases, the O_2 level is actually at its excess concentration listed in Table 3.1, however this concentration was subtracted from the data to clearly show O_2 production and depletion. Common trends can be seen for all materials including a quick initial increase in O_2 production followed

by a sharp negative dip in concentrations. This initial jump could be a couple things, including O_2 buildup behind the pressure wave associated with the dropping of the biomass into the reaction chamber. Another explanation is that initial decompositions of the biomass quickly release O_2 before it reacts with other gases to form compounds. The sharp dip is associated with this reaction of O_2, C, and H_2 to create compounds such as CO, CO_2, and H_2O. The most negative instantaneous concentrations of O_2 can be seen with corn at a temperature of 796°C, which is about 200% lower than any other concentration. Corn also produced the highest CO yield at this temperature (796°C) as well. The lowest point of each temperature series corresponds to the peak production of CO seen in Figure 3.1. The highest instantaneous concentrations and overall yields of CO correspond to the highest O_2 depletion concentrations.

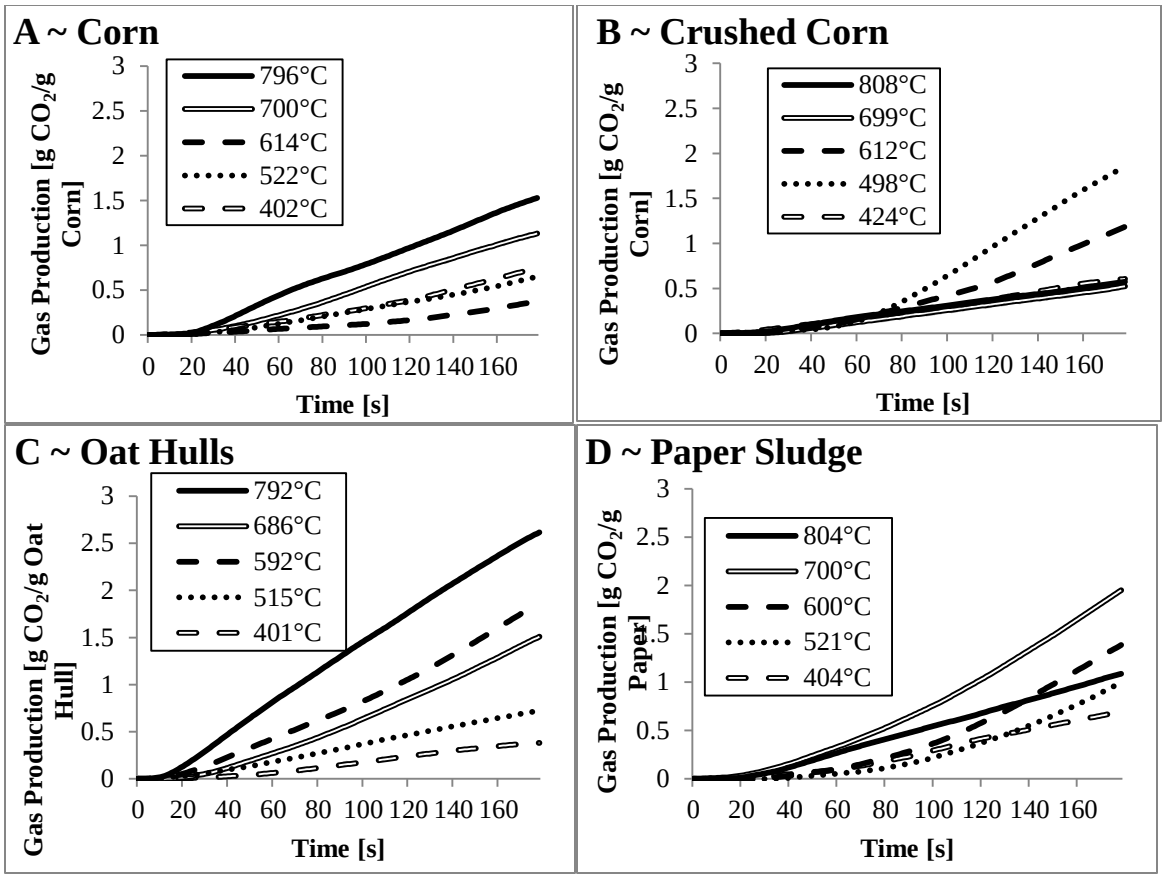

Figure 3.4: CO_2 production versus time for A) corn kernels, B) crush corn kernels, C) oat hulls, and D) paper sludge

Figure 3.5 clearly shows the magnitude of O2 depletion among the different materials; however, to better understand the O2 production through pyrolysis, Figure 3.6 is used. In Figure 3.6, the O2 concentrations have been normalized where the initial concentration is one and the minimum for each data series is zero. All values above one show the production of O2 from pyrolysis. Using this method, crushed corn produces the most O2 in comparison to the depletion, about 350% higher than the initial concentration at a temperature of 498°C. This temperature maximizes O2 production; however, it also produces minimal CO. Since CO is the main energy carrier of this process (in the absence of char reduction), crush corn pyrolysized at 498°C is non-ideal. Operating

temperatures that produce the least O2 also produce the most CO. However, low operating temperatures that produce little O2, generally produce very little CO. Therefore, CO and O2 production are not inversely proportional to each other but their relation is temperature driven.

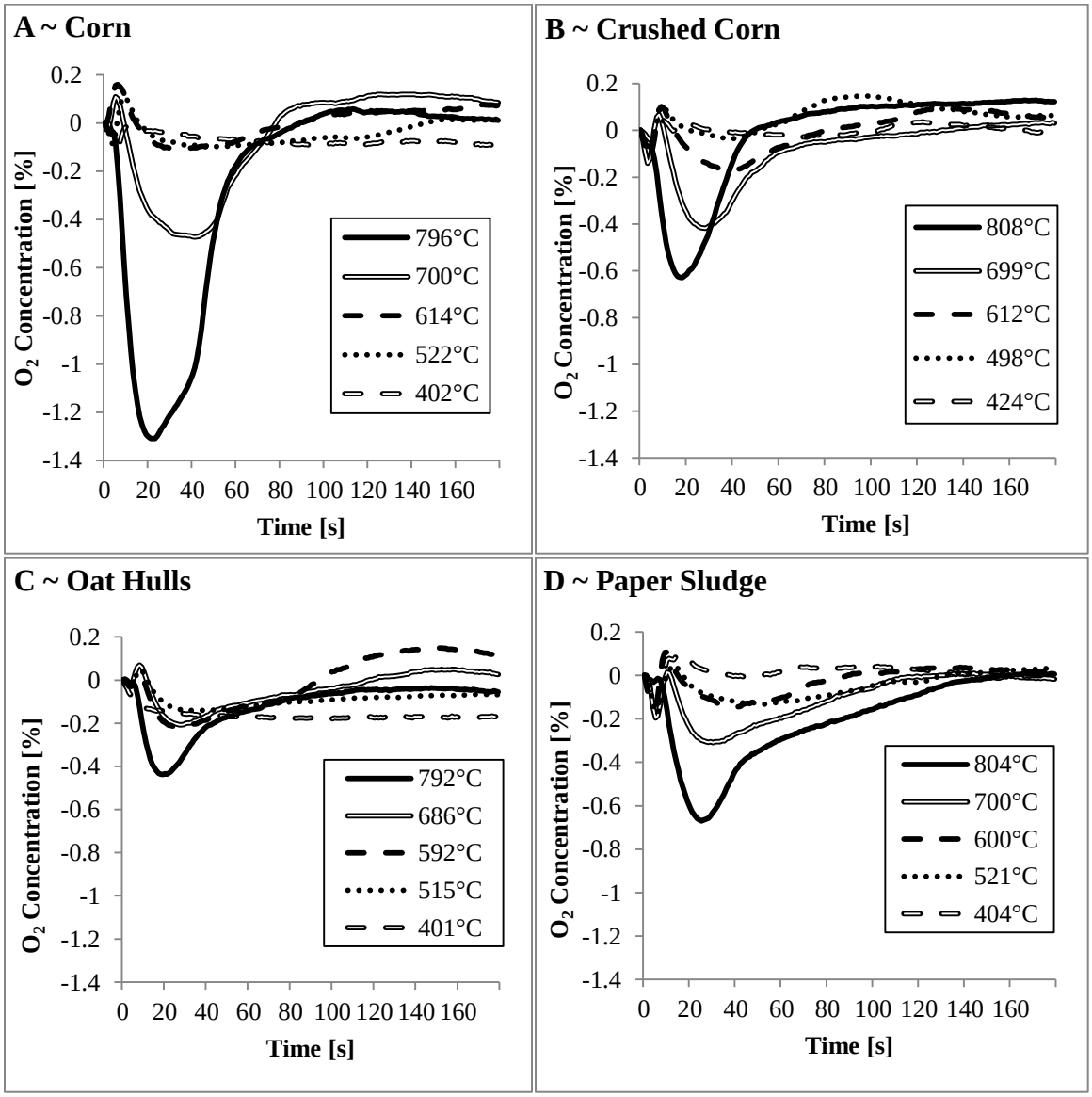

Figure 3.5: O_2 concentration evolution versus time for A) corn kernels, B) crush corn kernels, C) oat hulls, and D) paper sludge

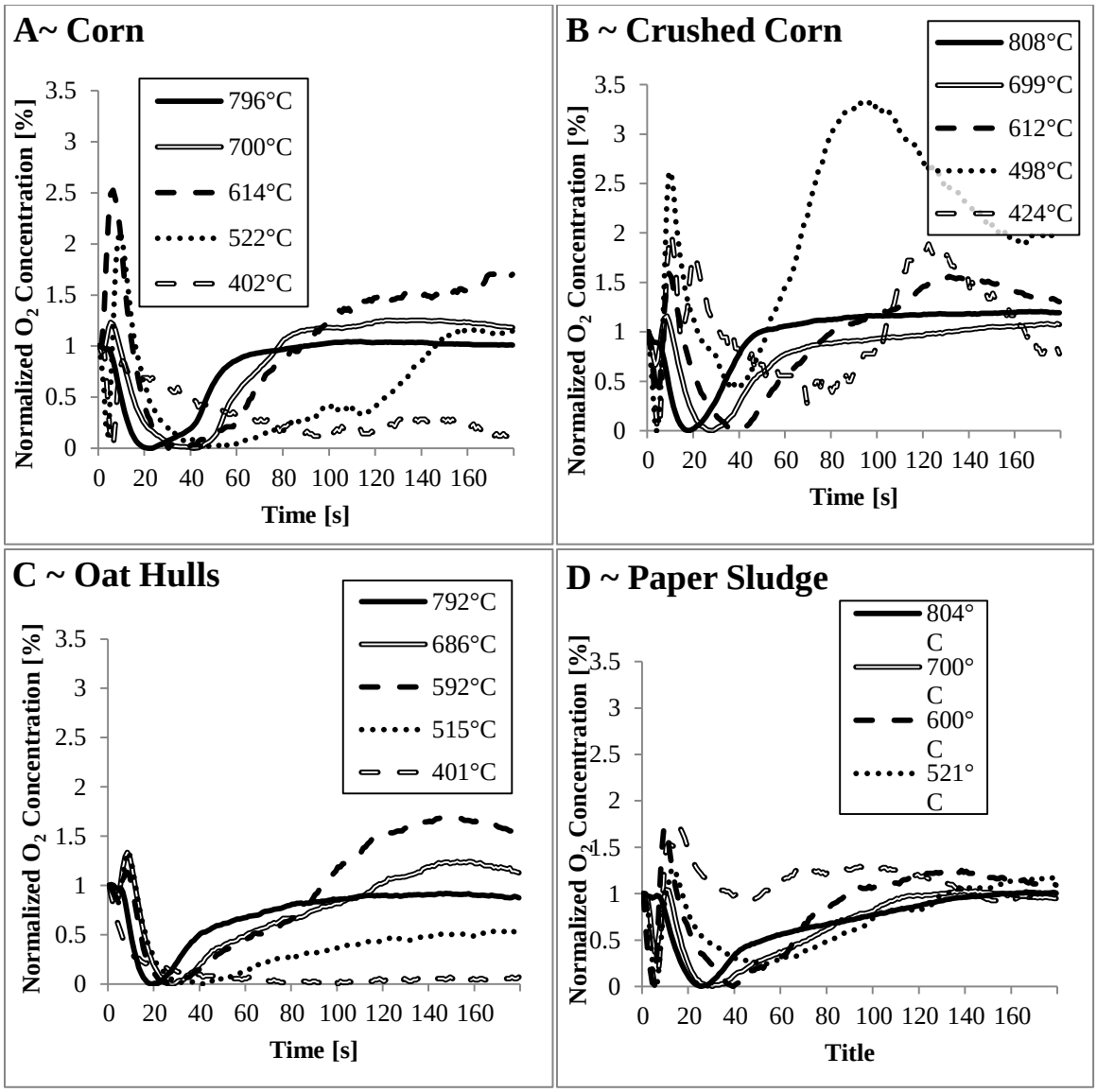

Figure 3.6: Normalized instantaneous O2 concentrations versus time for A) corn kernels, B) crush corn kernels, C) oat hulls, and D) paper sludge

3.5 Methane and Hydrogen Measurements

The H_2 produced from the biomass was measured during all tests; however, negligible H_2 was detected. The lack of H_2 production was found to be explained by the gas residence time which is ~ 0.2 seconds. This gas residence time is short in comparison to modern industrial systems and other experimental configurations which can be

significantly longer [6, 13, 17, 18, 19 - 22]. Longer residence times allow heavier hydrocarbons and CH_4 to be broken down into their simplest forms, increasing the hydrogen production. For gasification processes not included in this study, which include char breakdown and char gasification, will detect significantly higher concentrations of H_2. Small particles and rapid heating rates have also been found to reduce the H_2 produced [13, 23] and both conditions are present in the current work. It was anticipated that H_2 production would be negligible and these suspicions were confirmed.

While negligible H_2 was detected, more CH_4 was produced than was detectable by the ENMET EX-5120 IR CH_4 sensor used. The range for this sensor was from 0 – 5% of the total volume and in some instances, more than measureable concentrations of CH_4 were detected, generally at temperatures between ~ 700 - 800°C for corn kernels. However, these readings were inconclusive due to the erratic measurements. Every other sample was either higher than the sensor could measure (> 5%) or it measured a negligible amount. The reason for the erratic CH_4 measurements is unknown however, the sensor was replaced days before the final tests were conducted and was calibrated correctly. The main speculation for the CH_4 sensor problems is conditioning of the pyrolysis gas. After pyrolysis, the gas enters an ice bath where it is cooled before it enters multiple particulate filters followed by the sensors. The purpose of the particulate filters is to remove the tar produced in pyrolysis along with any water or large unknown particles. Numerous sensors have been replaced over the life of this experiment due to tar buildup within the sensor and it is believed that the CH_4 IR sensor is extremely sensitive to these contaminants, causing erratic measurements.

3.6 Comparison of Results to Other Studies

To validate the results of this study, the total CO yield was compared to other similar studies and can be seen in Figure 3.7. The most notable difference between this work and others is that the CO yields are significantly higher than previous studies at The University of Iowa by DeCristofaro in 2009 and Lenert in 2008. DeCristofaro's and Lenert's experiments operated at similar operating conditions; however, the gasifying agent was pure heated N_2. No O_2 was present in the stream. As discussed earlier, excess O_2 in the gasifying agent enhances CO production, increasing yields. Therefore, it was expected that the results would be significantly higher than yields measured by DeCristofaro and Lenert. In the figure, the oat hulls show similar but higher yields than previous works while other materials, in particular corn, show significantly higher yields. This again can be contributed to the O_2 concentration in the stream and the high energy density of corn. Dupont examined biomass gasification at high temperatures (1073 – 1273 K) with pure N_2 streams and the yields are again smaller than those measured in this work. Fushimi examined the effect of heating rate of the gasification of a biomass at 700°C and found similar yields similar to those found in this work for oat hulls.

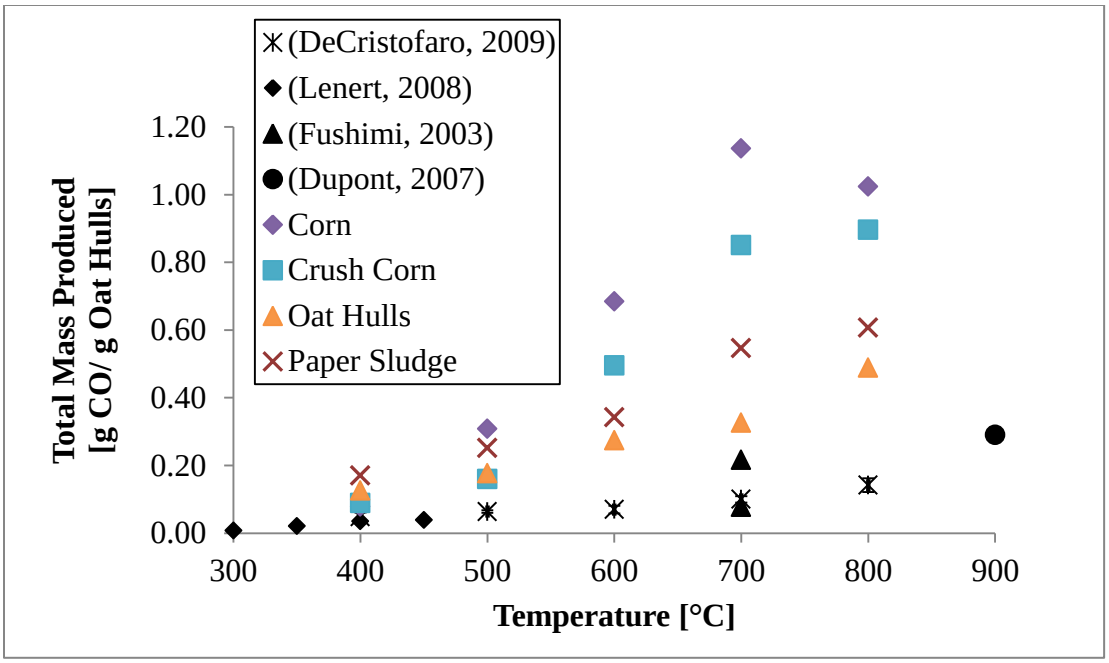

Figure 3.7: CO yield vs. temperature for present work and other studies

DeCristofaro also examined the effect of excess O_2 in the gasification stream and found that CO yields greatly benefitted from small concentrations of O_2 (up to 10%). However, an optimum value of O_2 was never calculated due to time constraints. This work however, used similar methods to increase the O_2 concentration (increasing the ratio of O_2 to CH_4 in the heating torch) and found an optimal value of 30% undiluted excess O_2, or between 2 – 8% when mixed with the N_2 gasification stream. In Figure 3.8, DeCristofaro's results are compared to those found in this study for oat hulls at 700°C with identical operating conditions with the exception of the O_2 concentration. The red series represents the current work at the optimum O_2 concentration while DeCristofaro varied the O_2 levels from 0 – 20.95% (air). As expected, the optimal O_2 concentration provides the highest CO yield. Also, yields at 4 and 10% O_2 are similar to those found in this work whereas at 0% O_2, the maximum CO yield ¼ of those at the optimal O_2

concentration. This comparison confirms that higher yields can be expected from O_2 concentrations greater than 0% in the gasification stream.

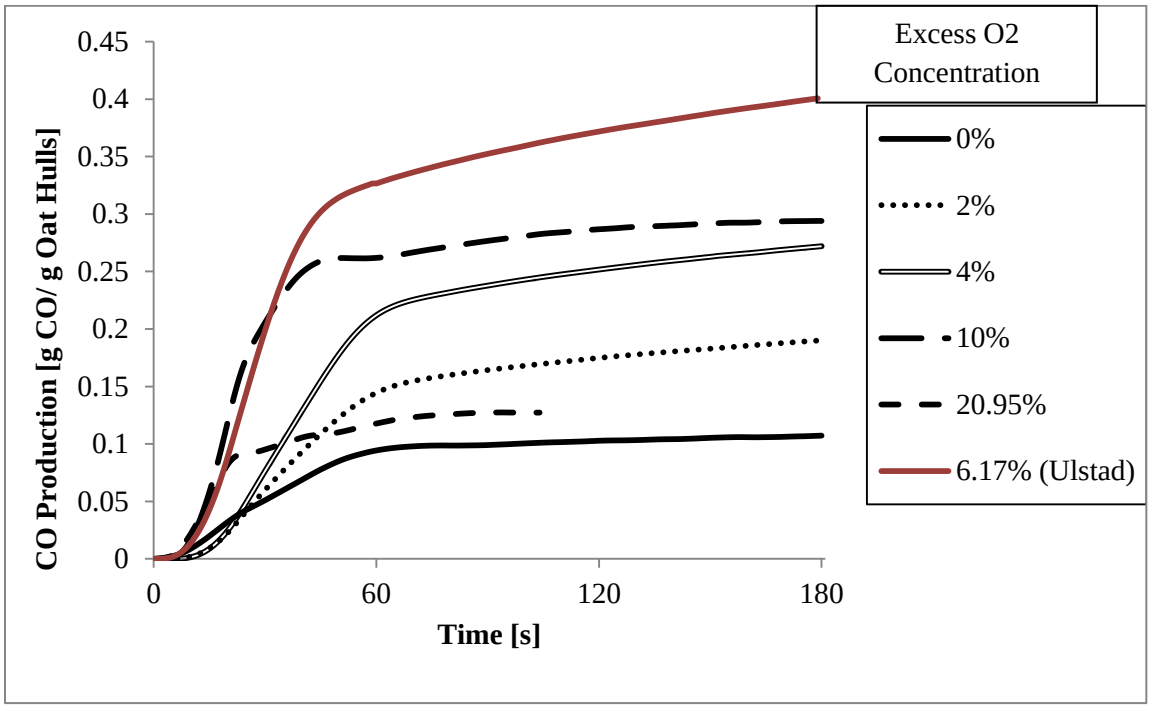

Figure 3.8: Comparison with DeCristofaro's findings for CO production at changing O_2 volumes ranging from 0 - 20.95%

3.7 Uncertainty

Error and uncertainty arise is several distinct ways for the present experimental apparatus and testing methodology. The mass flow meters have an absolute error of up to 5%, but repeated testing has shown that repeatability and relative error tend to be ~1%. Biomass mass error is less than 1%. Gas sensor error is 5%, although the CO_2 signal had to be measured with the products of the heating torch, resulting in a CO_2 signal error of ~20%. Temperature error would result from spatial separation between the thermocouple and the biomass sample, which varies for each biomass. For corn, the variation is ~20°C

since the material only extends 1-2 cm away from the thermocouple. The oat hulls and paper sludge are less dense, and hence extend up to 6 cm away, corresponding to a 60°C drop in gasification temperature at the upper most extant of the biomass.

CHAPTER 4

CONCLUSIONS AND FUTURE WORK

4.1 Conclusions

Biomass gasification is a process by which biomass waste products are converted into energy through incomplete combustion. The gasification process is notoriously difficult to simulate due to the complex chemistry associated with its three stages: drying, pyrolysis, and char gasification. These stages tend to overlap and can occur simultaneously throughout the biomass in a packed bed of a modern gasifier. This work attempts to understand a sub-process of gasification known as pyrolysis. During pyrolysis, the majority of the volatiles stored within the biomass are released during its decomposition through heat. To better understand this process, multiple biomasses (corn kernels, paper sludge, and oat hulls) were gasified long enough for complete pyrolysis (~3 minutes) at chamber temperatures ranging from 400 - 800°C. From this low temperature pyrolysis, the gas evolution of CO, CO_2, H_2, CH_4, and O_2 was measured to understand how the gas is released. This knowledge can later be translated to CFD models simulating gasification to more accurately describe pyrolysis and its effects on gasification.

The gas evolution of CO from pyrolysis was measured and it was found that the peak gas evolution increased with an increase in temperature. The time to peak evolution significantly increased with a decrease in temperature for all biomasses except for oat hulls, where the time to peak gas evolution remained fairly constant at about 25 – 30 seconds. The largest gas evolution was measured for crushed corn kernels to at ~800°C; however, the gas evolution amplitudes were similar across both whole and crushed corn kernels. Pyrolysis occurred slower for the whole corn kernels than the other biomasses

and this is believed to be related to the size of the whole kernel (which is much *larger* than the other biomasses) and its relative surface area exposed to the heated N_2 stream (which is much *smaller* than the other biomasses). The total CO gas production of the gasification gas was also studied by integrating the total CO gas evolved. Whole corn kernels produced higher yields at all temperatures in comparison to the other biomasses. Crushed corn kernels produced similar but lower yields. Oat hulls and paper sludge, both with small particle sizes, produced about half as much CO as corn. The particle size of the biomass affects the gasification products as seen from the CO gas evolution for whole and crushed corn.

The CO_2 gas evolution was also measured and the results were less conclusive. Due to the large volume of CO_2 produced by the torch, the CO_2 measured from gasification was noisy and no trends could be determined. Larger volumes of CO_2 were measured for paper sludge and oat hulls than for the corn kernels. This could be again related to the low density and particle size of paper sludge and oat hulls.

A small concentration of O_2, not burned through the combustion of the torch, was mixed with the heated N_2 stream used to gasify the material. The O_2 concentration was measured and it was found that this excess O_2 played a significant role in the production of CO. Large O_2 depletions coincided with large CO productions. If O_2 was produced in large volumes, the CO production was much lower. Particle size again played a role in the gas evolution of O_2. Whole corn kernels, with the largest particle size, experience the largest O_2 depletion. Crushed corn gasification resulted in less CO production and lower O_2 depletion than whole corn kernels. The other lighter biomasses also experienced low O_2 depletion and CO production in comparison to corn.

No H_2 was measured due to the short residence time as expected. Modern gasifiers with longer residence times (~30 minutes) will measure significant volumes of H_2; however, for pyrolysis, it is rare to measure large volumes. CH_4 was measured, however, the measurements were inclusive due to the humidity and tar within the gasification products, causing damage to the sensor.

The results from this work are directly applicable to current CFD gasification models lacking pyrolysis data. This process is generally ignored due to the lack of data available for the pyrolysis stage. The results can be summarized through numerical models and inputted into models for the specific materials. Most CFD modelers require specific forms for their equations based on the software used and modeler preference. Due to this, the numerical models were not constructed and are left to the modeler. The hope is that more accurate CFD gasification models can be constructed from these results, aiding in the design and understanding of gasification systems.

4.2 Future Work

The future of this work depends on major changes in the design of the heating system. The dual heating system, an electric heater and torch, employed by this work enables a high heating rate and a wide temperature range. However, the torch produces more than heat. CO_2 and H_2O produced from the torch increase the noise floor of the torch requiring a larger sensor range with lower accuracy. The CO_2 measurements are victims of this reality and the results are too noisy for trends to develop. The produced H_2O mixes with the biomass tars and creates a brown liquid that causes damage to the sensors. An ideal heating system would employ a single electric flow heater, capable of high heating rates and temperatures of ~1000℃. The electric flow heater applies heat

from electrical resistance in wire heating elements through convection. This heating system does not produce permanent gases such as CO_2 and H_2O, making it ideal for capturing results from the pyrolysis process. However, large electric heating systems were too expensive at the start of this project. Future work and funding should focus on developing a new heating system without a torch.

A second major recommended change from the author is to purchase a multicomponent FTIR gas analyzer, such as the Gasmet DX-4000. This Fourier transform infrared spectrometer, can analyze wet, corrosive gas streams for numerous complex gas mixtures including those measured in this work and other heavier hydrocarbons. This system and other similar sensors are heavily utilized in gasification work due to their accuracy, versatility, and ability to measure up to 50 different compounds. Again, this system is extremely expensive and ~$50,000 of additional funding is necessary.

To better analyze the results, quality particle size measurements and relative surface area calculations are needed. In addition to density and the biomass composition (lignin and cellulose fractions), a method to predict the gasification products for *any* biomass could be accurately determined. Lastly, an attempt to increase the solid residence time and sample size is necessary to more accurately mimic the conditions of a modern gasifier.

REFERENCES

[1] The University of Iowa: Pioneering Technology for Utilizing Biomass Fuels. Brochure. 2007.

[2] Kumar A, Jones D D, Hanna M A: Thermochemical Biomass Gasification: A Review of the Current Status of the Technology. *Energies* 2009, 2 (3), 556-581.

[3] Basu P, Kaushal P: Modeling of Pyrolysis and Gasification of Biomass in Fluidized Beds: A Review. *Chemical Product and Process Modeling* 2009, 4, 1-45.

[4] Nikoo M B, Mahinpey N: Simulation of biomass gasification in fluidized bed reactor using ASPEN PLUS. *Biomass and Bioenergy* 2008, 32, 1245 – 1254.

[5] Sadaka S: Pyrolysis *Sungrant Bioweb*. Sungrant Initive, 15 Nov. 2008. Web.

[6] Dupont C, Commandre J M, Gauthier P, Boissonnet G, Salvador S, Schweich D: Biomass pyrolysis experiments in an analytical entrained flow reactor between 1073 K and 1273 K. *Fuel* 2008, 87 (7), 1155-1164.

[7] Lee D H, Yang H P, Yan R, Liang D T: Prediction of gaseous products from biomass pyrolysis through combined kinetic and thermodynamic simulations. *Fuel* 2007, 86 (3), 410-417.

[8] Xiao X, Le D D, Li L, Meng X, Cao J, Morishita K, Takarada T: Catalytic steam gasification of biomass in fluidized bed at low temperature: Conversion from livestock manure compost to hydrogen-rich syngas. *Biomass and Bioenergy* 2010, 34, 1505 -1512.

[9] Gautam G, Adhikari S, Bhavnani S: Estimation of Biomass Synthesis Gas Composition using Equilibrium Modeling. *Energy and Fuels* 2009, 24, 2692-2698.

[10] Dai X W, Wu C Z, Li H B, Chen Y: The fast pyrolysis of biomass in CFB reactor. *Energy &Fuels* 2000, 14 (3), 552-557.

[11] Barneto A G, Carmona J A, Galvez A, Conesa J A: Effects of the Composting and the Heating Rate on Biomass Gasification. *Energy & Fuels* 2009, 23 (1), 951-957.

[12] Pletka R, Brown R C, Smeenk J: Indirectly heated biomass gasification using a latent heat ballast. Part 2: modeling. *Biomass and Bioenergy* 2001, 20, 307-315.

[13] Fushimi C, Araki K, Yamaguchi Y, Tsutsumi A: Effect of heating rate on steam gasification of biomass. 1. Reactivity of char. *Industrial & Engineering Chemistry Research* 2003, 42 (17), 3922-3928.

[14] Lui C, Yan B, Chen G, Bai X S: Structures and Burning Velocity of Biomass Derived Gas Flames. *International Journal of Hydrogen Energy* 2010, 35, 542 – 555.

[15] The Ohio State University: Seed Treatment. Bulletin

[16] DeCristofaro E: Gas Evolution from Biomass Gasification and Pyrolysis. Master's Thesis. The University of Iowa, 2009

[17] Xianwen, Dai, Chuangzhi W, Haibin L, Yong C. *Energy & Fuels* 14 (2000): 552-57.

[18] Zanzi R, Sjostrom K, Bjornbom E. *Biomass and Bioenergy* 23 (2002): 357-66.

[19] Fagbemi L, Khezami L, Capart R, *Applied Energy* 69 (2001): 293-306.

[20] Zanzi, Rolando, Sjostrom K, Bjornbom E, *Fuel* 75 (1995): 545-50.

[21] Kinoshita C M, Wang Y, Zhou J, Journal of Analytical and Applied Pyrolysis 29 (1994): 169-81.

[22] Yanik, Jale, Kornmayer C, Saglam M, Yuksel M, Fuel Processing Technology 88 (2007): 942-47.

[23] Zabaniotou A., Ioannidou O, *Fuel* 87 (2008): 834-43.